First Observation of Normalised Emittance Reduction through Ionization Cooling

DRAFT - MICE Internal

C. T. Rogers

Muon ionization cooling is a technique by which muon beam emittance may be reduced in order to improve the beam transmission and luminosity. Ionization cooling is a key component of proposed muon facilities such as the Muon Collider and Neutrino Factory but until now has never been demonstrated in practice.

In this paper, the effect of focussing of muons onto an energy absorber, using a very high acceptance solenoid assembly, is described. The muon phase space distribution is measured upstream and downstream of the focus. The muons are studied both with and without an energy absorber. The emittance of the muon ensemble is shown to decrease in the presence of an energy absorber and the phase space density is shown to increase, indicating that the beam has been successfully cooled.

1 Introduction

1.1 Ionisation Cooling

Ionization cooling [**?**] is the only known technique that can cool a muon beam on a timescale competitive with the muon lifetime [**?**] [**?**] [**?**] [**?**]. Muon cooling has never been demonstrated previously. In ionization cooling, a beam is passed through an absorber causing energy to be lost due to ionization of atomic electrons. This yields a reduction in normalized transverse emittance. Multiple Coulomb scattering from atoms causes an increase in angular divergence of the beam, and hence emittance growth. The change in normalized RMS emittance $\varepsilon_\perp$ in distance dz is [**?**]

$$\frac{d\varepsilon_\perp}{dz} \approx -\frac{\varepsilon_\perp}{\beta^2 E_\mu}\left\langle\frac{dE}{dz}\right\rangle + \frac{\beta_\perp (13.6\,\mathrm{MeV/c})^2}{2\beta^3 E_\mu m_\mu X_0} \tag{1}$$

where $\beta_\perp$ is the transverse optical Twiss function, βc, E_μ, m_μ are the particle velocity, energy and mass, and X_0 is the radiation length. There exists an equilibrium RMS emittance ε_{eqm}

$$\varepsilon_{eqm} \approx \frac{1}{2m_\mu}\frac{13.6^2}{X_0}\frac{\beta_\perp}{\beta\left\langle dE/dz\right\rangle} \tag{2}$$

at which $d\varepsilon_\perp/dz = 0$. If a beam with emittance below equilibrium is incident on an absorber, its emittance increases on passage through the absorber. Otherwise the emittance decreases.

1.2 The Muon Ionisation Cooling Experiment

MICE Step IV [**?**] [**?**] consists of a transfer line to bring particles from the ISIS synchrotron at Rutherford Appleton Laboratory to the cooling experiment. The cooling equipment consists of a section of a solenoid

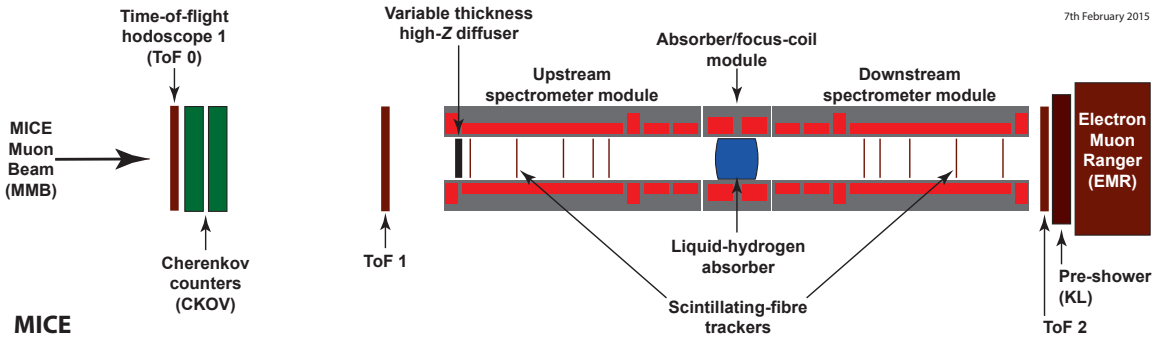

Figure 1: The MICE apparatus.

focussing ionization cooling cell. Detectors, placed upstream and downstream of the emittance reduction apparatus, measure the momentum, position and species of particles entering and leaving the cooling channel, enabling the measurement of change in normalized beam emittance of the ensemble. A schematic of the apparatus is shown in fig. 1.

1.3 Transfer Line

Pions are created by dipping a titanium target into the ISIS proton synchrotron. A dedicated transfer line has been constructed to transport the resultant particles to the cooling apparatus [**?**] [**?**] [**?**]. The incoming particle momentum can be selected by varying the field in a pair of dipoles. Higher magnetic field selects higher particle momentum. A series of tungsten and brass irises are positioned in the transfer line, enabling the selection of different emittances for the ensemble.

Up to around 100 particles are observed per second. MICE accumulates data in runs, each run consisting of a single experimental configuration and lasting of order hours. Several runs are taken for each solenoid configuration. MICE has taken data over thousands of runs, with many different configurations.

1.4 Cooling Channel

The cooling channel consists of three superconducting solenoid modules [**?**] [**?**]. Two spectrometer solenoid modules each generate a region of uniform field in which diagnostic trackers are situated and a matching region that transports the beam from the solenoid to the focus coil module. The focus coil module, positioned between the solenoids, provides additional focussing to increase the angular divergence of the beam at the absorber, improving the amount of emittance reduction that can be achieved.

The absorber was a 21 litre vessel. When filled, the absorber presents 350 mm of liquid Hydrogen along the experimental axis. Liquid hydrogen was chosen as an absorber material as it provides less multiple Coulomb scattering for a given energy loss, due to the smaller electric charge of the nucleus. Containment of the Hydrogen was provided by a pair of thin Aluminium windows. An additional pair of windows provided secondary containment in case of failure of the primary containment windows.

1.5 Diagnostic Apparatus

Upstream of the cooling apparatus, two time-of-flight detectors (TOFs) [**?**] [**?**] enable the measurement of particle velocity, which is validated by a threshold Cerenkov counter [**?**]. Scintillating fibre trackers,

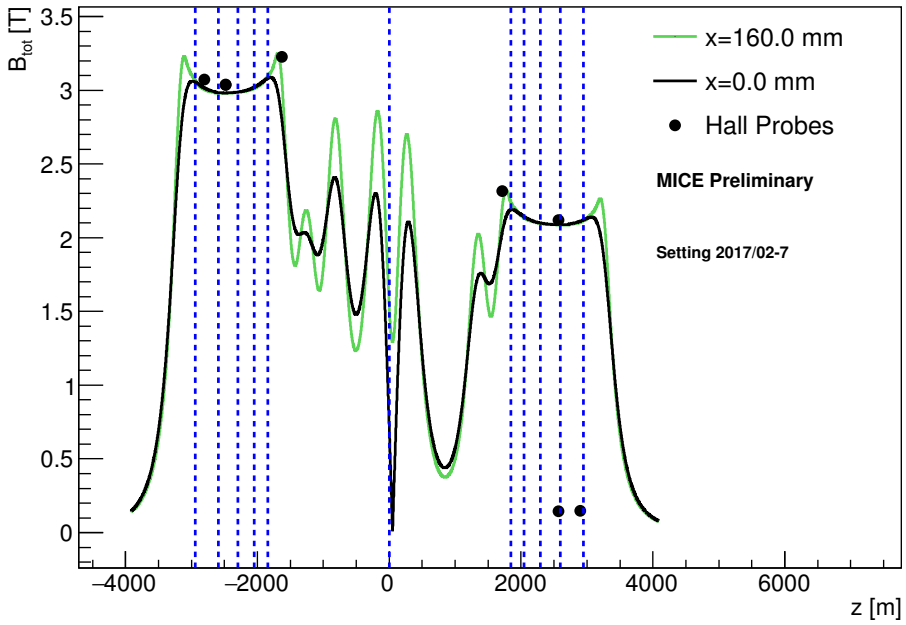

Figure 2: Modelled magnetic field for the configuration on the axis and with 160 mm horizontal displacement from the axis. Hall probes, situated 160 mm from the beam axis, show a 2 % discrepancy with the model. Dashed lines show position of the tracker stations and absorber.

positioned either side of the absorber module, enable the measurement of particle position and momentum upstream and downstream of the absorber. Further downstream an additional TOF detector, a KLOE Light pre-shower detector and Electron Muon Ranger enable rejection of electron impurities.

The trackers consist of 5 stations [**?**] [**?**]. Each station consists of 3 views, each view rotated by 120° with respect to the previous view. Each view consists of 2 layers of scintillating fibres. Gangs of 7 scintillating fibres are read out together by cryogenically operated Visible Light Photon Counters, enabling the position of incident particles to be measured with a resolution of 0.3 to 0.4 mm. The trackers are situated in uniform 3 T fields such that particles make a helical path. The magnitude of the field is measured using Hall probes situated in the region of the tracker. By measuring the radius and pitch of the helix, the momentum of the particle can be deduced. The trackers have sufficient redundancy to enable the track reconstruction to be internally validated in order to estimate the efficacy of the reconstruction. The uncertainty on the momentum of each track is around 1-2 MeV/c.

Each TOF consists of two planes. Each TOF plane is made up of a number of scintillator slabs. Photomultiplier tubes at either end of the TOF slabs produce a signal when particles pass through the TOF. The time at which muons pass through the apparatus can be measured with a resolution of 60 ps.

1.6 Operation of the Equipment

In this paper the evolution of phase space density is reported for a single configuration of the cooling magnets, '2017-02 7'. The cooling channel magnet set currents and the beam optical parameters assuming no beta-beating in the upstream spectrometer solenoid are listed in table 1. A model of the magnetic field in this configuration is shown in fig. 2.

The transfer line settings were varied to mimic different beam conditions. Results from four transfer line

Table 1: Magnet parameters and other information for 2017-02 7. The cooling channel was powered in flip mode, meaning that SSU and the upstream coil in FC had positive polarity while the downstream coil in FC and SSD had negative polarity.

Setting	2017-02 7
Full absorber runs	9946 to 9972
Full Start time	12/10/2017 11:59
Full End time	14/10/2017 12:20
Empty absorber runs	10014 to 10077
Empty Start time	18/10/2017 14:34
Empty End time	23/10/2017 09:28
Nominal FC $\beta_\perp$ [mm]	WHAT BETA FUNCTION?
Nominal momentum [MeV/c]	140
SSU Center Coil [A]	205.7
SSU Match Coil2 [A]	168.25
SSU Match Coil1 [A]	191.0
FC Coil [A]	129.24
SSD Match Coil2 [A]	195.72
SSD Center Coil [A]	144.0

configurations are reported, with the accumulated muon sample having nominal emittances of 3 mm, 4 mm, 6 mm and 10 mm at momenta around 140 MeV/c in the upstream spectrometer solenoid. These configurations are denoted '3-140', '4-140', '6-140' and '10-140' respectively.

1.7 Simulation

The cooling channel was modelled using various codes. Simulated particles based on a representative model of the pion yield from the target were transported through to the upstream edge of TOF1 using G4Beamline [**?**]. Downstream of this region, MAUS [**?**] was used to model particle transport and the response of the MICE detectors to the incoming beam.

2 Sample Selection

Update for revised cuts e.g. extrapolation cuts and global recon. List sample sizes.

2.1 Particle events

The MICE data acquisition system was set to trigger if TOF1 received simultaneous hits in a given slab. The trigger enables readout of the diagnostics during a short trigger window. All data acquired during this period is associated together and known as a particle event.

Signals in the same detector are associated into space points, for signals that are consistent with a particle passing through a given spatial region, and tracks, for signals that are consistent with a particle with a given momentum passing through a number of space points. The full reconstruction chain is described in [**?**].

2.2 Sample Selection

Particle events are selected for analysis according to a number of different criteria. Two samples are considered: the upstream sample is selected based on criteria in the upstream detector system only; the downstream sample is selected from the upstream sample, based on additional criteria in the downstream detector system. Because the upstream sample is selected based on measurements in the upstream detector system, the upstream sample is independent of any stochastic processes occurring in the absorber.

The sample selection criteria are detailed in Table **??** together with the number of events surviving each cut. The criteria are described in detail below.

Table 2: The sample selection criteria are listed sequentially, in the order that the selection was made. The number of events surviving the selection and all preceding selections is listed for each of the data runs studied in this note.

cut	2017-2.7 3-140 lH2 empty	2017-2.7 3-140 lH2 full	2017-2.7 6-140 lH2 empty	2017-2.7 6-140 lH2 full	2017-2.7 10-140 lH2 empty	2017-2.7 10-140 lH2 full	2017-2.7 3-140 LiH	2017-2.7 3-140 None	2017-2.7 6-140 LiH	2017-2.7 6-140 None	2017-2.7 10-140 LiH	2017-2.7 10-140 None
all events	171016	183035	166998	272188	202390	349494	240396	250992	286274	256894	471965	375988
tof 1 sp	164936	177064	161150	264382	189475	332706	231587	241795	276621	248748	441852	355633
tof 0 sp	132005	146186	124753	217087	139713	262363	183288	191029	213920	196733	326715	271817
scifi tracks us	50732	56756	85717	146438	74251	138217	70331	72679	147602	134002	174896	144374
scifi nan us	50732	56756	85717	146438	74251	138217	70331	72679	147602	134002	174896	144374
chi2 us	46457	51472	76992	129199	67114	122946	64058	66406	132585	120897	157499	130091
scifi fiducial us	46421	51408	76936	129111	66655	122084	64006	66346	132494	120794	156424	129131
delta tof01	26790	30340	37903	72016	34345	74575	38854	38377	71809	59444	91368	65311
tof01	25518	27638	34540	59829	27291	55848	36083	36769	60979	54897	66763	52552
p tot us	9200	9710	13562	22752	7172	14099	12776	13703	23208	21557	16991	13715
global through tku tp	9197	9697	13506	22569	6667	12149	12773	13700	23048	21501	14983	13031
global through tof1	9197	9697	13506	22569	6667	12149	12773	13700	23048	21501	14983	13031
global through tof0	9197	9697	13506	22569	6667	12149	12773	13700	23048	21501	14983	13031
upstream aperture cut	8992	9488	13299	22191	5185	9786	12371	13226	22667	21114	12057	10196
upstream cut	8992	9488	13299	22191	5185	9786	12371	13226	22667	21114	12057	10196
scifi tracks ds	8820	9207	12851	21358	4835	9055	12134	13064	21937	20526	11178	9666
scifi nan ds	8820	9207	12851	21358	4835	9055	12134	13064	21937	20526	11178	9666
chi2 ds	8573	8964	12508	20833	4716	8857	11820	12646	21354	19916	10918	9376
scifi fiducial ds	8573	8964	12508	20833	4716	8857	11820	12646	21354	19916	10918	9376
p tot ds	8512	8898	12408	20668	4681	8784	11724	12556	21236	19778	10854	9312
downstream cut	8512	8898	12408	20668	4681	8784	11724	12556	21236	19778	10854	9312
downstream aperture cut	4633	5076	7575	12522	2197	3906	6712	6954	12931	11957	4935	4308
tof2 sp	4633	5076	7575	12522	2197	3906	6712	6954	12931	11957	4935	4308
global through tkd tp	4633	5076	7575	12522	2197	3906	6712	6954	12931	11957	4935	4308
global through tof2	4474	4846	7251	11914	2103	3670	6425	6743	12292	11545	4609	4162
extrapolation cut	4474	4846	7251	11914	2103	3670	6425	6743	12292	11545	4609	4162

Table 3: Upper and lower bound of TOF cuts for different beamline settings.

Beamline	Lower Bound [ns]	Upper Bound [ns]
3-140	27.0	32.0
6-140	27.0	31.0
10-140	27.0	30.0

2.3 Upstream Sample

Cuts applied to the upstream sample are described below.

- One TOF1 Space Point: Events have exactly one space point reconstructed in TOF1.
- One TOF0 Space Point: Events have exactly one space point reconstructed in TOF0.
- One TKU Track: Events have exactly one track reconstructed in TKU, with finite position and momentum and associated error matrices.
- TKU χ^2 per degree of freedom: The reconstructed χ^2 per degree of freedom in TKU is required to be less than 10. The χ^2 per degree of freedom of events in each sample is shown in fig. 6.
- TKU fiducial cut: Events are required to have a maximum radial excursion in TKU less than 150 mm. The maximum radial excursion of the track is estimated assuming a helical trajectory between tracker stations. The maximum radial excursion of events in each sample is shown in fig. **??**.
- TKU Momentum: Events are required to have momentum reconstructed by TKU between 135 and 145 MeV/c. The momentum of events in each sample is shown in fig. 13. Discuss low momentum bulge?
- TOF01 Time: Pions and electrons in the momentum selection described above have a quite different time-of-flight between TOF0 and TOF1 to muons. Events are required to have time-of-flight between TOF0 and TOF1 consistent with a muon in order to reject this background. The time-of-flight of events in each sample is shown in fig. 9. The velocity of particles upstream of the diffuser is faster for thicker diffuser settings, in order to yield a muon sample with momentum peaked around 140 MeV/c in TKU. In order to correctly reject impurities, the TOF01 cut is different for different beamline settings, as listed in table 3

Events which do not meet these criteria are not considered for analysis at all.

2.4 Downstream Sample

Cuts applied to the downstream sample are described below.

- In Upstream Sample: Events are required to be in the upstream sample to be considered in the downstream sample.
- One TKD Track: Events have exactly one track reconstructed in TKD.
- TKD Momentum: Events are required to have reconstructed momentum between 100 and 200 MeV/c. The momentum as reconstructed by TKD of events in each sample is shown in fig. **??**
- TKD χ^2 per degree of freedom: The reconstructed χ^2 per degree of freedom in TKD is required to be less than 10. The χ^2 per degree of freedom of events in each sample in TKD is shown in fig. 6.

Events which do not meet these downstream sample criteria are not considered for analysis. They may either have collided with the cooling channel aperture and been lost (scraping), or they may have been not observed by the detectors (inefficiency). Systematic correction and uncertainty due to detector inefficiency is discussed in Section [**?**].

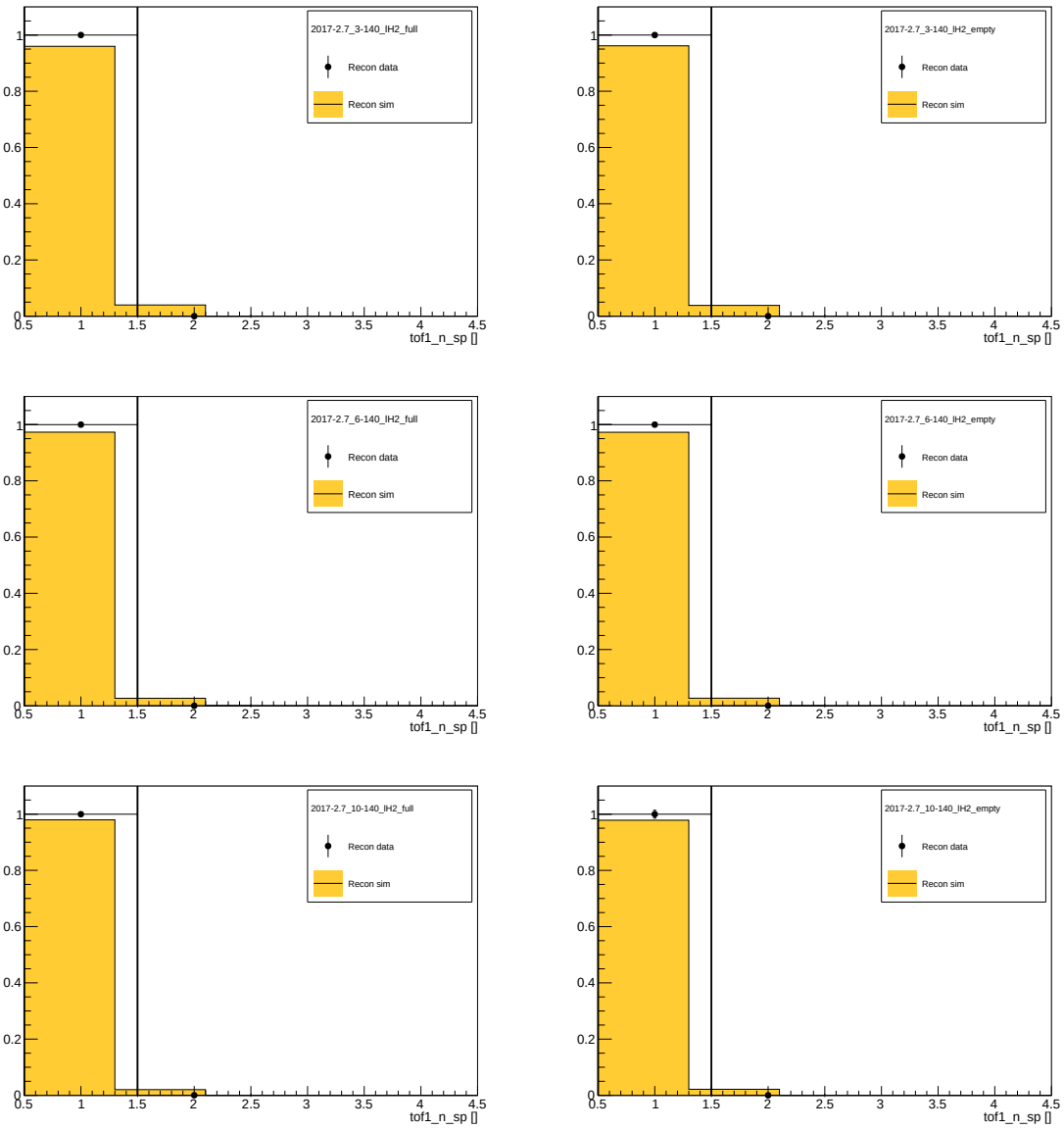

Figure 3: Number TOF1 space points.

3 Detectors

In this section, the resolution and efficiency of the detector systems is discussed. The reconstruction is validated both internally within each detector system, using the detector's internal redundancy, and by extrapolating reconstructed events between detectors.

3.1 Tracker

References

Two trackers, made up of five stations each with three planes of scintillating fibres are used to reconstruct the momentum of incoming particles. Particles make helical trajectories whose radius and wavelength vary according to the transverse and longitudinal momentum respectively. The radius of the helix is given approximately

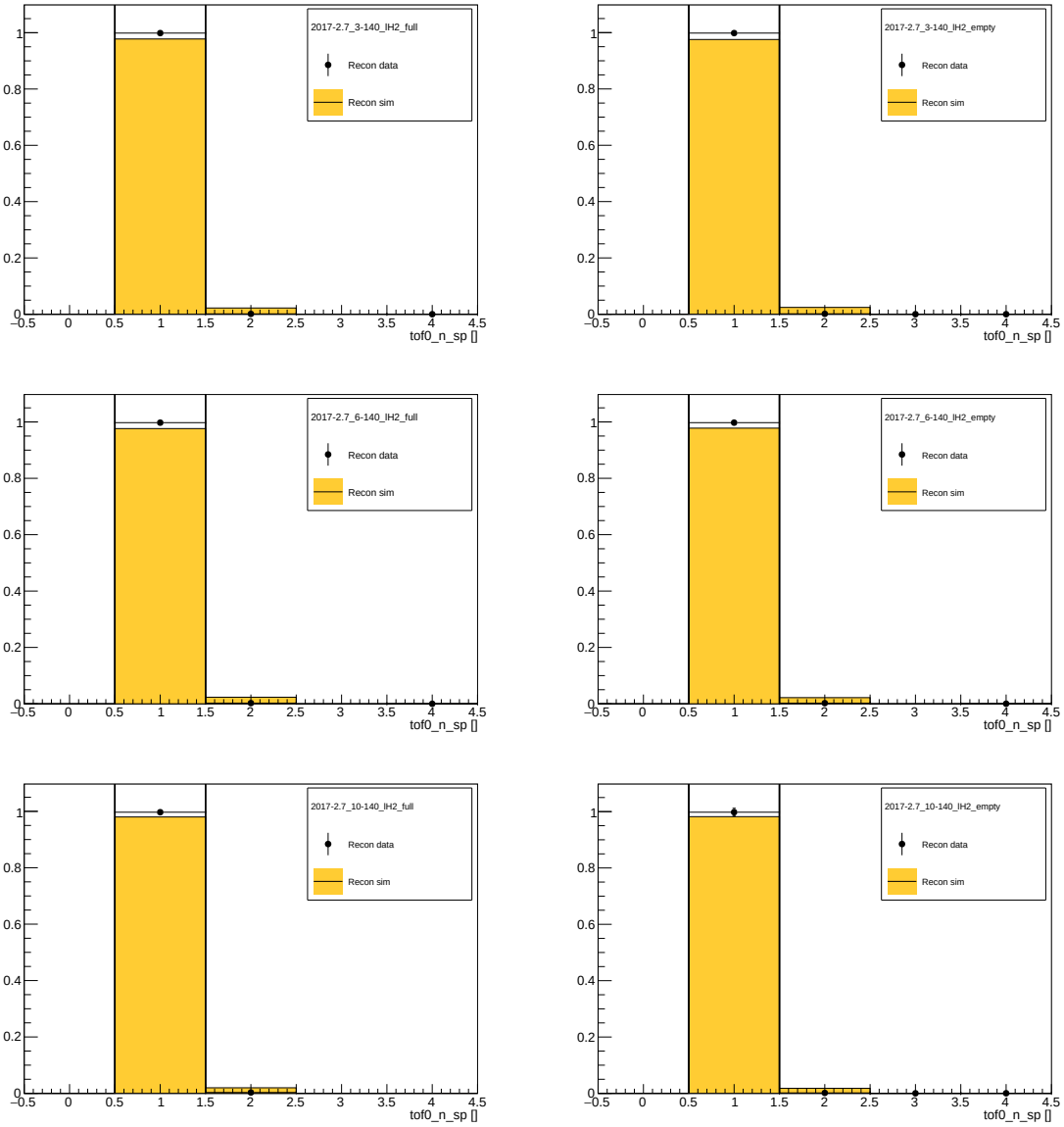

Figure 4: Number TOF0 space points.

by

$$r = \frac{p_t}{qB_z} \tag{3}$$

and the wavenumber by

$$k = \frac{qB_z}{p_z}. \tag{4}$$

Fitting is performed in several steps. Electronics signals arising from adjacent fibres are collected into clusters. The position of clusters in adjacent planes are collected to form a space point. A first-pass fit of a perfect helix to the space points is used for noise rejection and to seed a second-pass fit using a Kalman filter.

If the reconstruction is well-understood, the path of the reconstructed trajectory should match the position of the clusters. The χ^2 distribution of reconstructed tracks is shown in fig. **??**.

Add chi2 fit; add comment indicating chi2 fit is consistent.

In order to accurately reconstruct tracks the field must be well known. If the modelled field used in reconstruction differs from the actual field, a helix can be found but the longitudinal and transverse momenta will

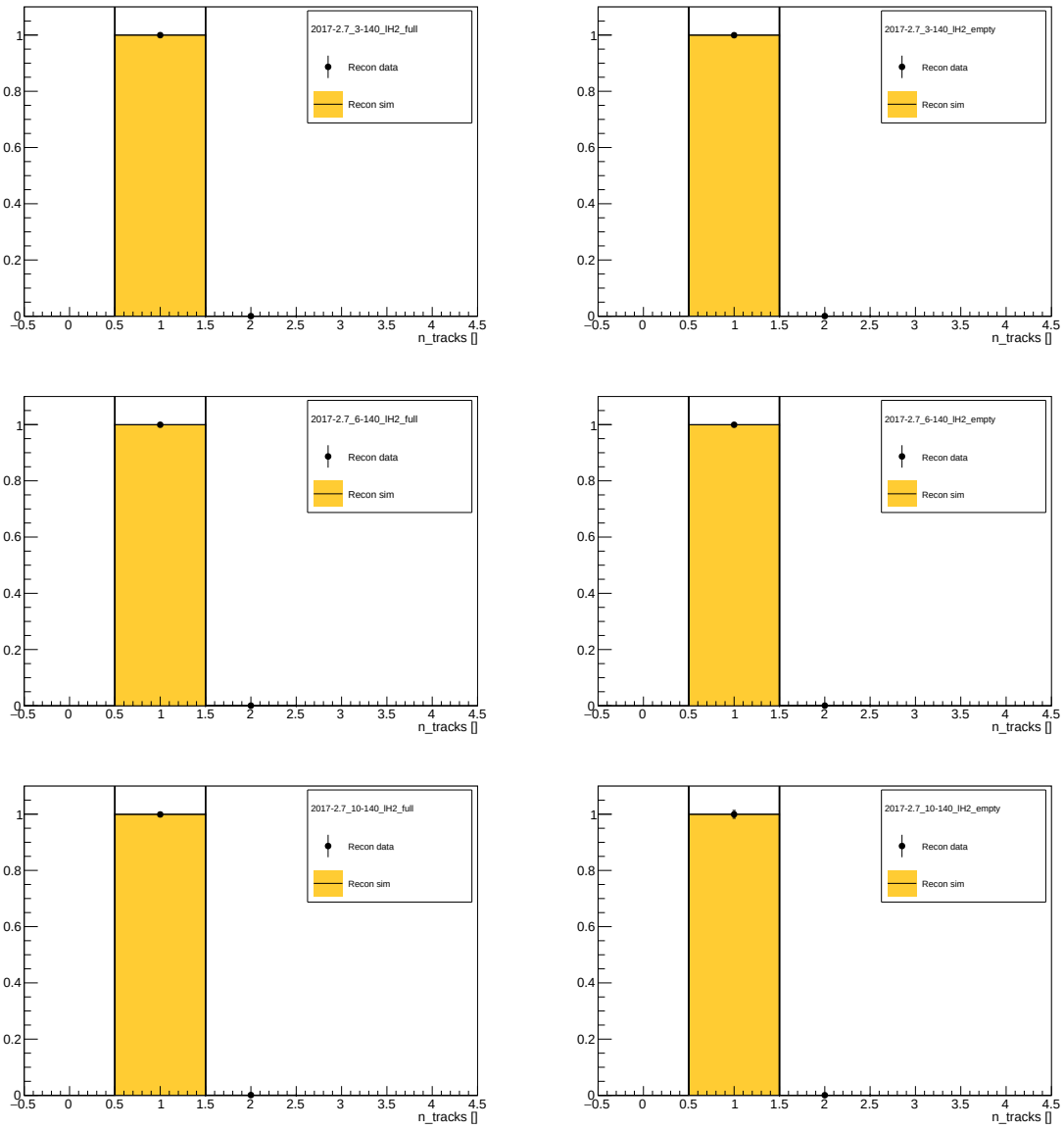

Figure 5: N tracks.

scale according to eq. (3) and eq. (4). In order to accurately reconstruct the field correctly it is essential to understand the measured field accurately.

The field in the tracker region was monitored during the data taking period by several Hall probes. The Hall probe measurement in the tracker region is shown in fig. 17 for several run periods, including the data taking periods under study in this paper. Reproducibility is demonstrated at better than 10^{-3} T level.

The measured fields are shown overlayed with the modelled field in the tracker region in fig. 18. There is some disagreement between the model and the hall probe readings, particularly in the fringe field of the magnets.

Proof that the efficiency is understood (and good); probably something like number of 5 point, 4 point tracks and demonstration that this is consistent with expected noise/dead channels? Look at straight tracks data?

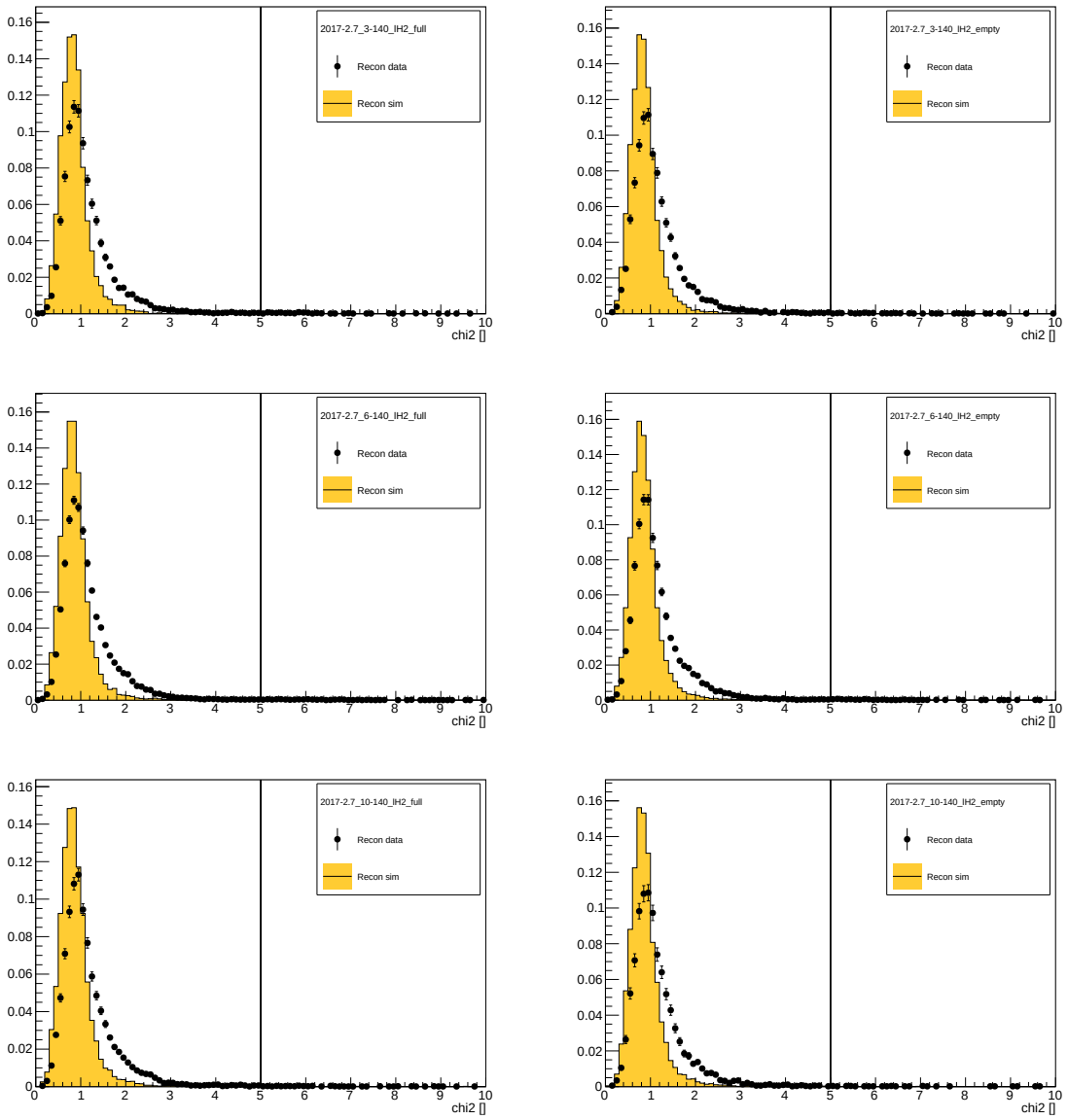

Figure 6: χ^2 per degree of freedom distribution in TKU for 3-140 beam (top), 6-140 beam (middle) and 10-140 beam (bottom). The left hand column shows data with full absorber; the right hand column shows data with empty absorber. The black line shows all events; red shows events in the upstream sample; green shows events in the downstream sample.

3.2 TOF

Description of the TOFs and reconstruction (few words but mostly citation).

Proof that the resolution is understood - e.g. plane 0 vs plane 1 for each TOF station.

4 Global reconstruction

The overall detector performance can be validated by considering the sample of events

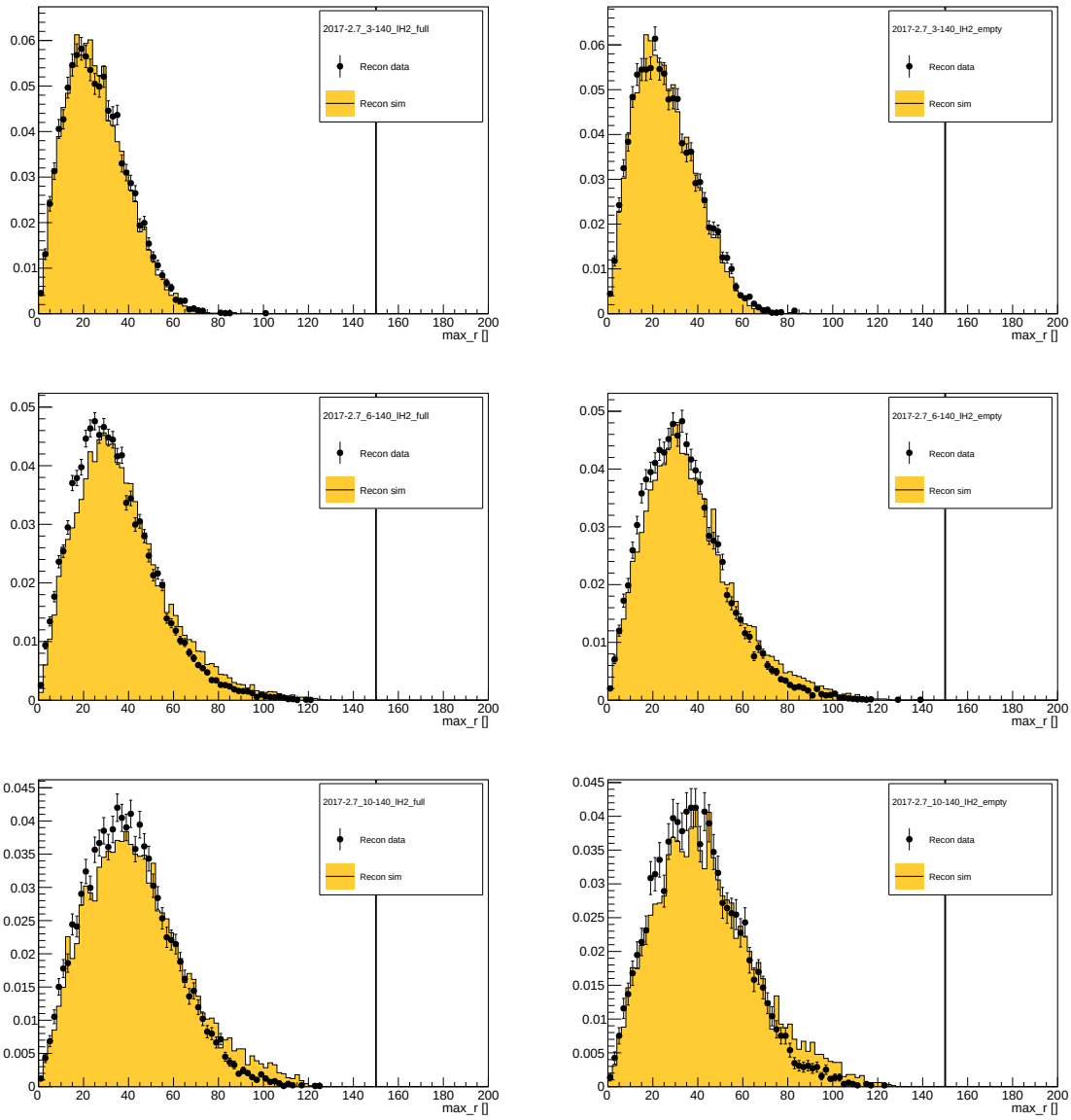

Figure 7: Maximum radius.

5 Cooling Channel

5.1 Magnets

The MICE cooling channel consists of 12 coils arranged in 3 magnet assemblies, SSU, FC and SSD.

Demonstrate stability of magnets over the operational period of the experiment - archiver and hall probes.

Demonstrate that we understand the magnetic channel; extrapolate tracks and show that they join up.

5.2 Absorber

Demonstrate that we understand the absorbers? Show that mean, RMS of extrapolated tracks is consistent with models for energy loss/straggling and MCS.

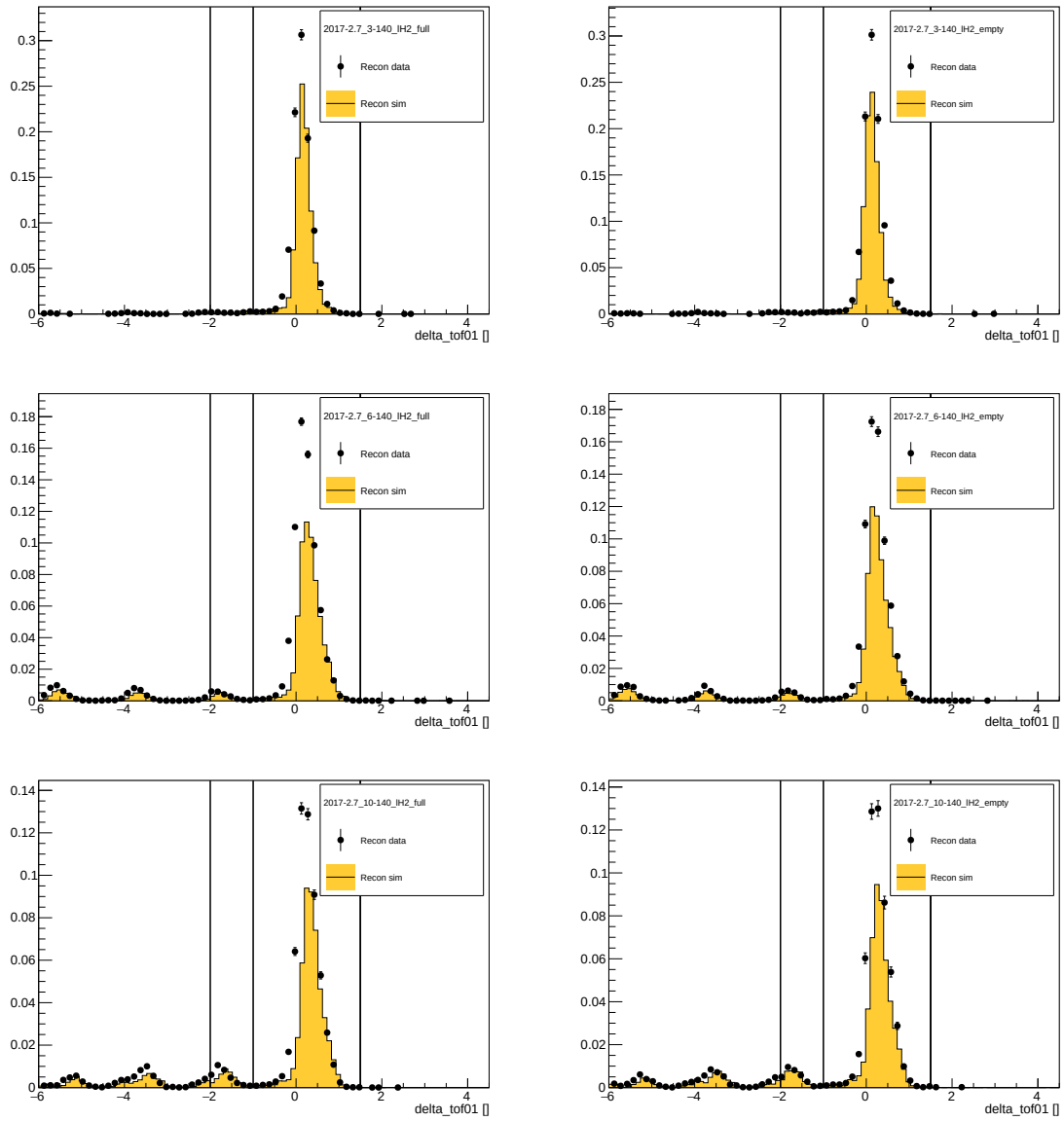

Figure 8: delta tof01.

6 Cuts

Author Rogers

Describe the sampling.

6.1 Good TOF0/TOF1 Cut

Reject events that don't get a clean signal in TOF0 and TOF1

6.2 Good TKU Cut

Reject events that don't get a clean signal in TKU.

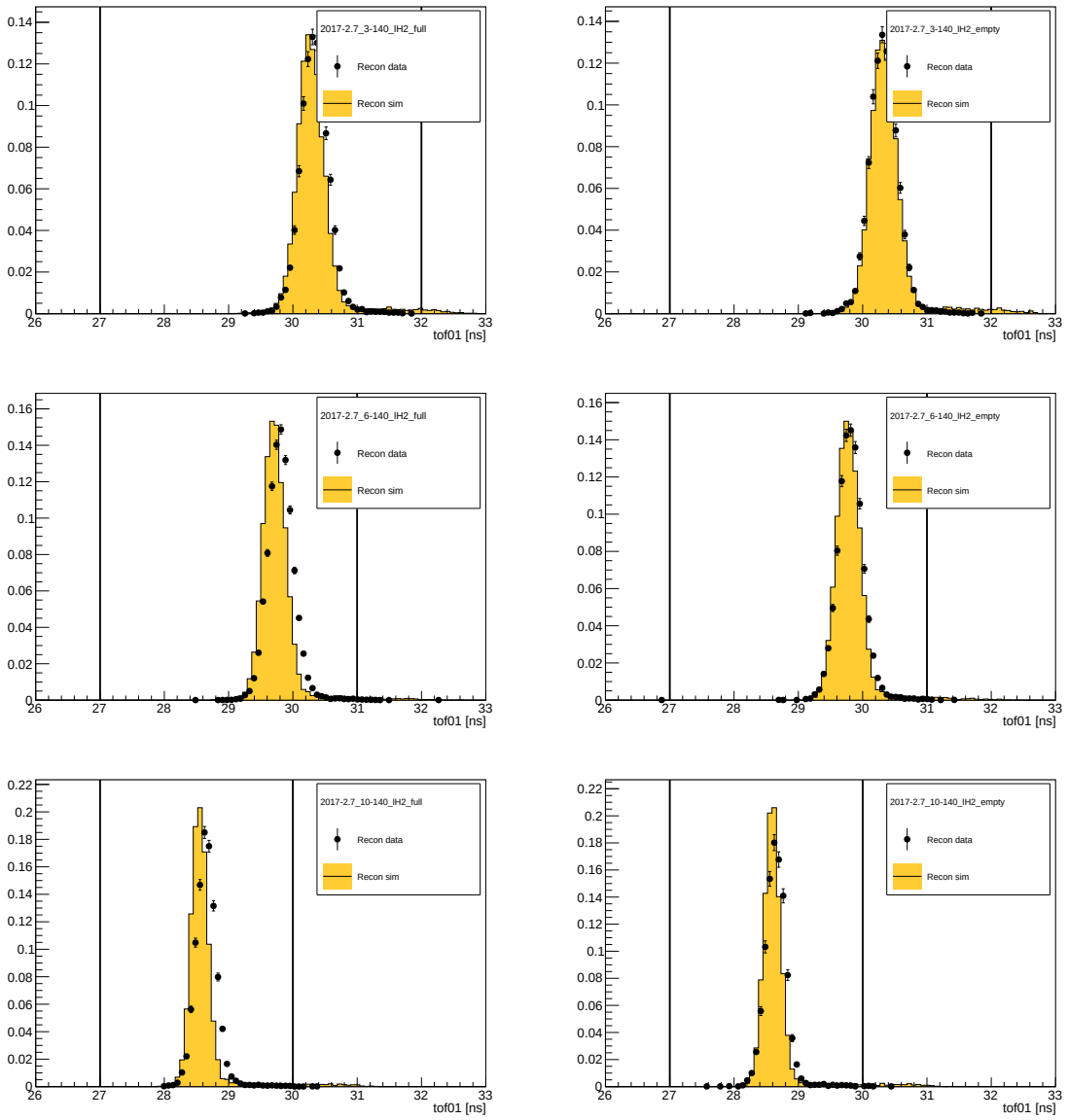

Figure 9: Time-of-flight measured between TOF0 and TOF1 for 3-140 beam (top), 6-140 beam (middle) and 10-140 beam (bottom). The left hand column shows data with full absorber; the right hand column shows data with empty absorber. The black line shows all events; red shows events in the upstream sample; green shows events in the downstream sample.

6.3 Aperture Upstream Cut

Reject muons going through upstream apertures (e.g. diffuser)

6.4 PID Cut

Reject muons based on TOF01 vs tracker. Show that this is consistent with PID cuts in other detectors. May need a whole section to discuss PID (e.g. do we want to go into Ckov, EMR, ”global PID”?), depending on how things go.

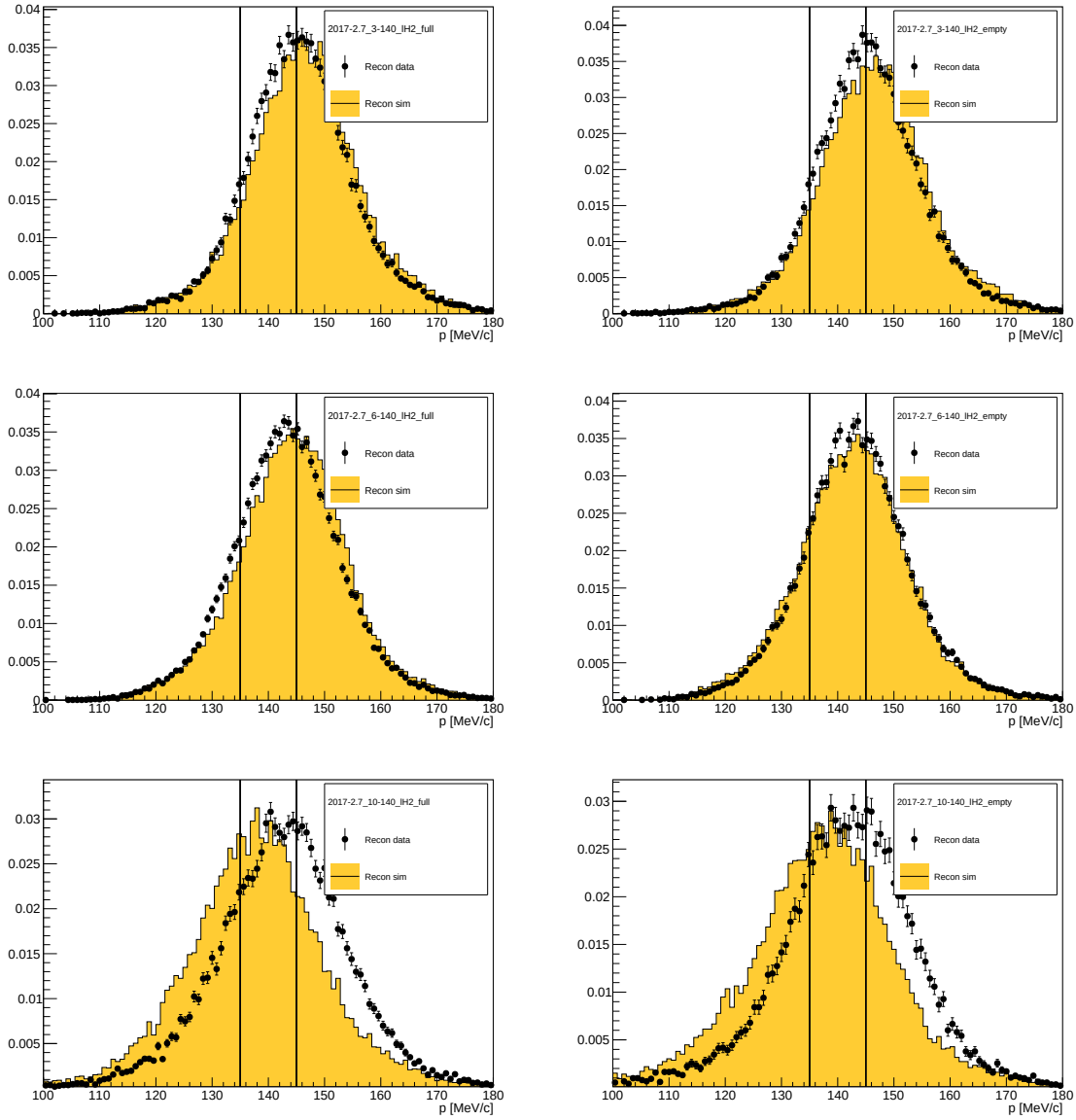

Figure 10: Momentum measured by TKU for 3-140 beam (top), 6-140 beam (middle) and 10-140 beam (bottom). The left hand column shows data with full absorber; the right hand column shows data with empty absorber. The black line shows all events; red shows events in the upstream sample; green shows events in the downstream sample.

6.5 TKU momentum cut

Reject muons based on TKU momentum; this is to reduce chromatic aberration.

6.6 Aperture cut

Depending on what plots go into the ”Results” section, we may want to make an aperture cut based on projected TKU tracks.

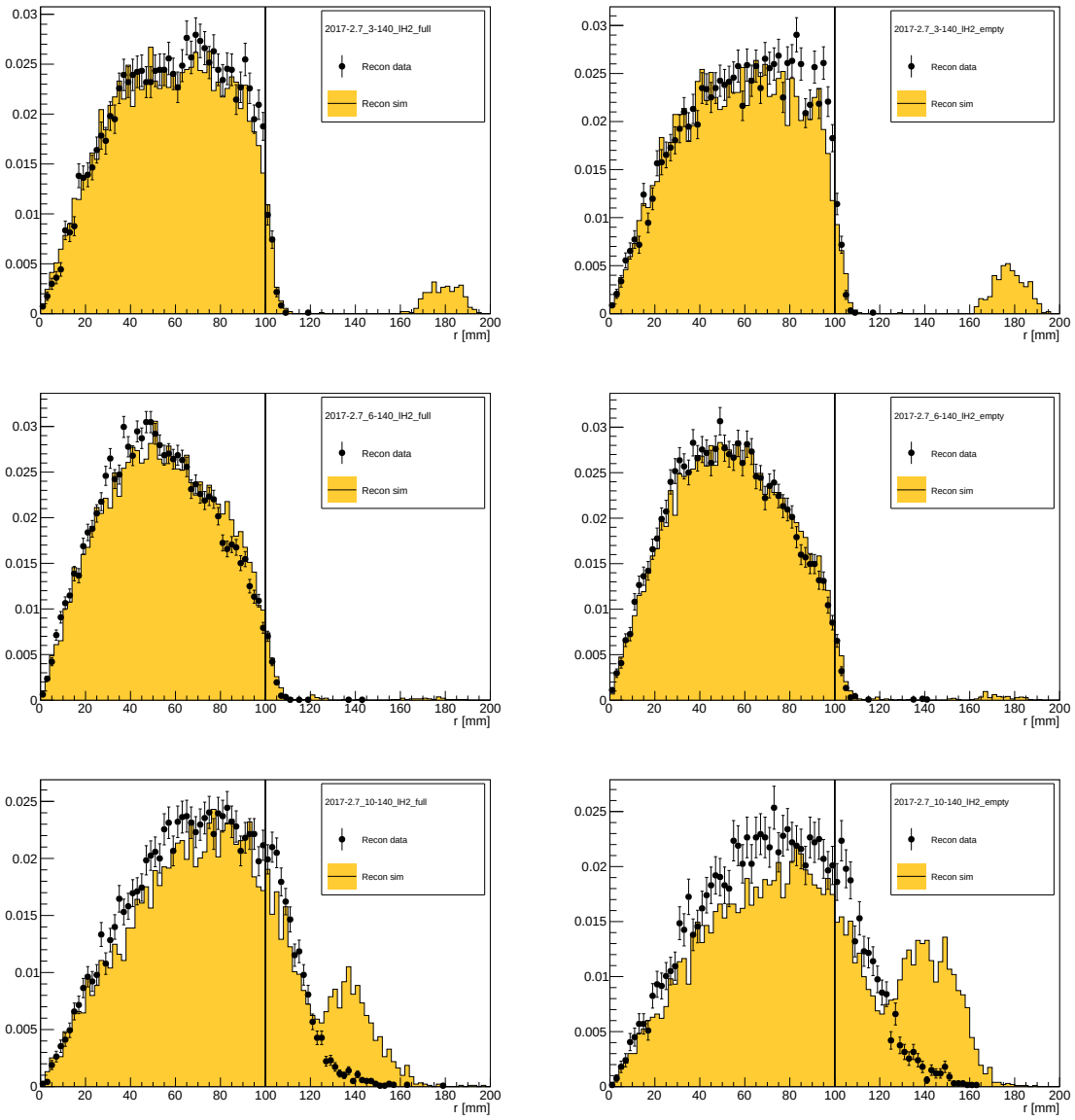

Figure 11: Diffuser cut

7 Results

Author Rogers

Describe the results.

7.1 Optics

Demonstrate that the optics is consistent with expectation i.e. projected beam upstream looks like measured beam downstream (beta functions?)

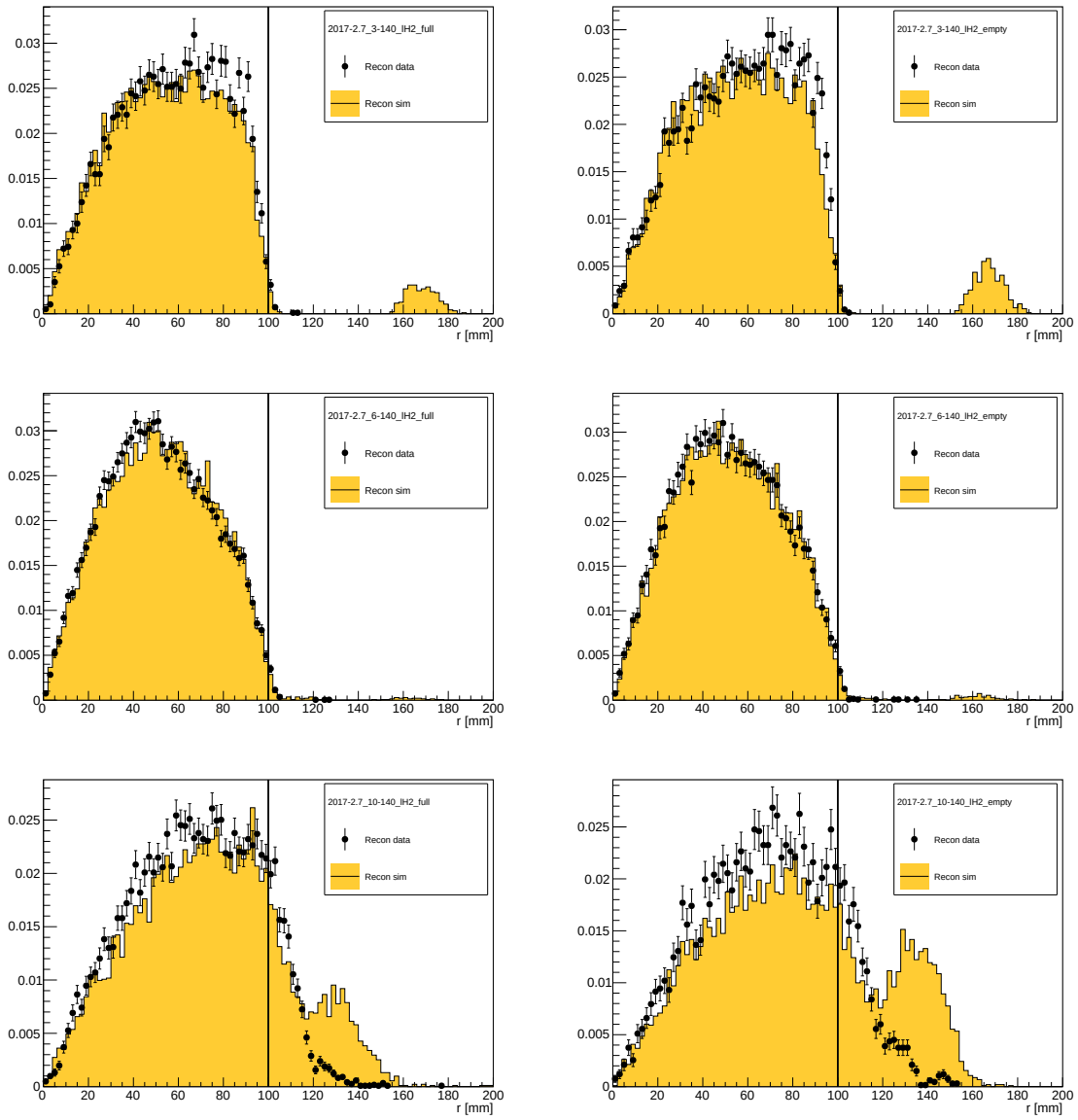

Figure 12: Momentum measured by TKU for 3-140 beam (top), 6-140 beam (middle) and 10-140 beam (bottom). The left hand column shows data with full absorber; the right hand column shows data with empty absorber. The black line shows all events; red shows events in the upstream sample; green shows events in the downstream sample.

7.2 Amplitude Distribution

The change in number of events upstream and downstream of the absorber is shown in **??** for empty and full configurations.

Show amplitude distribution upstream vs amplitude downstream.

8 Uncertainties

Discuss how we deal with various uncertainties. I imagine two classes of uncertainty: (i) those that affect the measurement; (ii) those that affect the model.

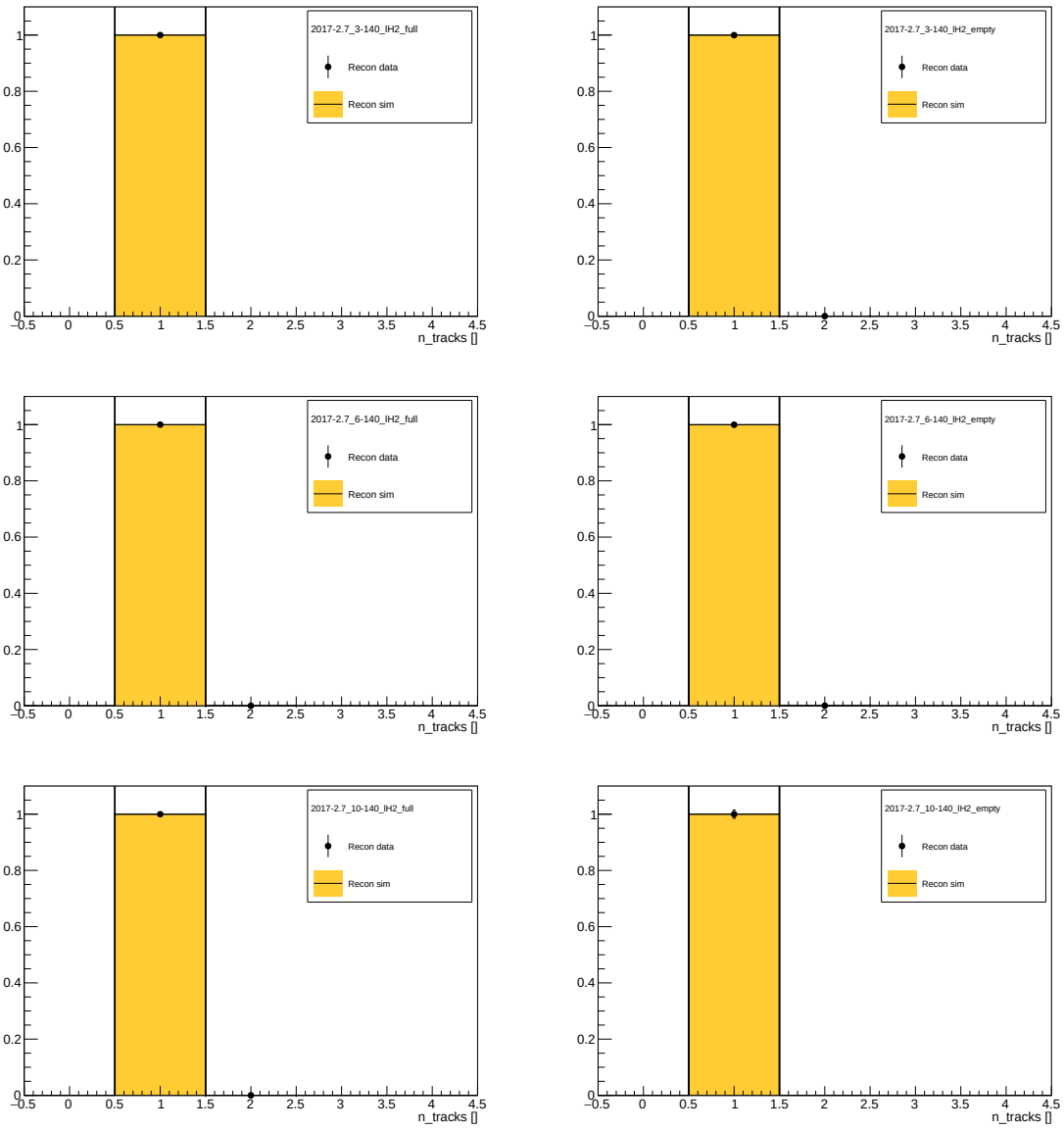

Figure 13: Momentum measured by TKU for 3-140 beam (top), 6-140 beam (middle) and 10-140 beam (bottom). The left hand column shows data with full absorber; the right hand column shows data with empty absorber. The black line shows all events; red shows events in the upstream sample; green shows events in the downstream sample.

8.1 Measurement Uncertainties

author: Rogers

The actual resolutions/etc have been introduced in the detectors section - so the job here is to make statistical/MC arguments about how they tie in to the data. E.g. how does TKD inefficiency affect emittance calculation?

- Detector resolution
- Detector noise and efficiency
- Magnetic field in reconstruction region

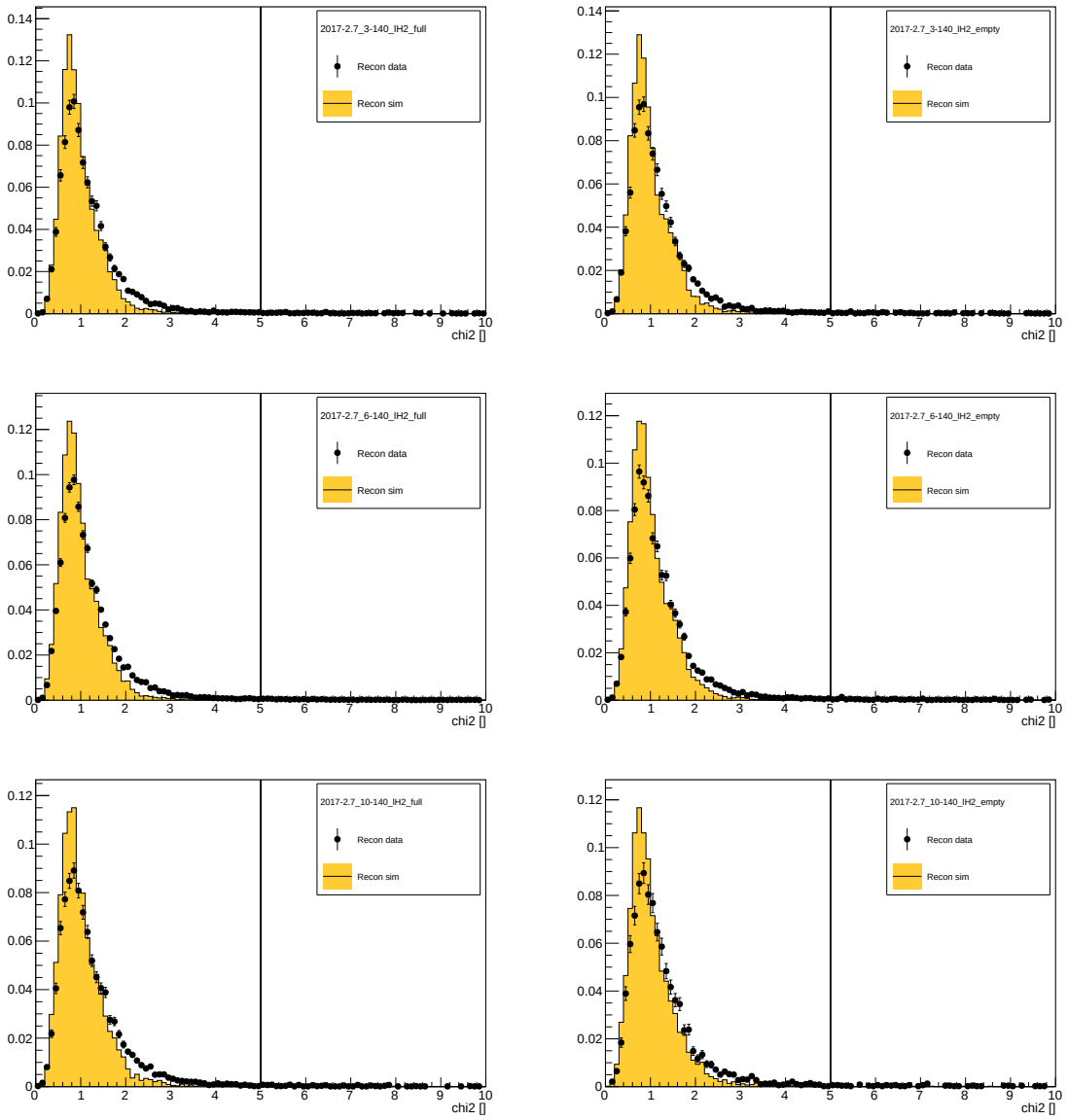

Figure 14: χ^2 distribution in TKD for 3-140 beam (top), 6-140 beam (middle) and 10-140 beam (bottom). The left hand column shows data with full absorber; the right hand column shows data with empty absorber. The black line shows all events; red shows events in the upstream sample; green shows events in the downstream sample.

8.2 Model Uncertainties

author: Liu

We measure a given emittance change and try to tie it into a model. The model can be wrong because e.g. the fields were wrong, the absorber was wrong, etc. We have following sources of uncertainty:

- Field uncertainty (alignment, current, etc)
- Absorber uncertainty (thickness, density, etc)
- Other material budget
- Not sure, maybe if we are projecting upstream tracks we should include the uncertainty on the upstream measurement? This is a bit circular...

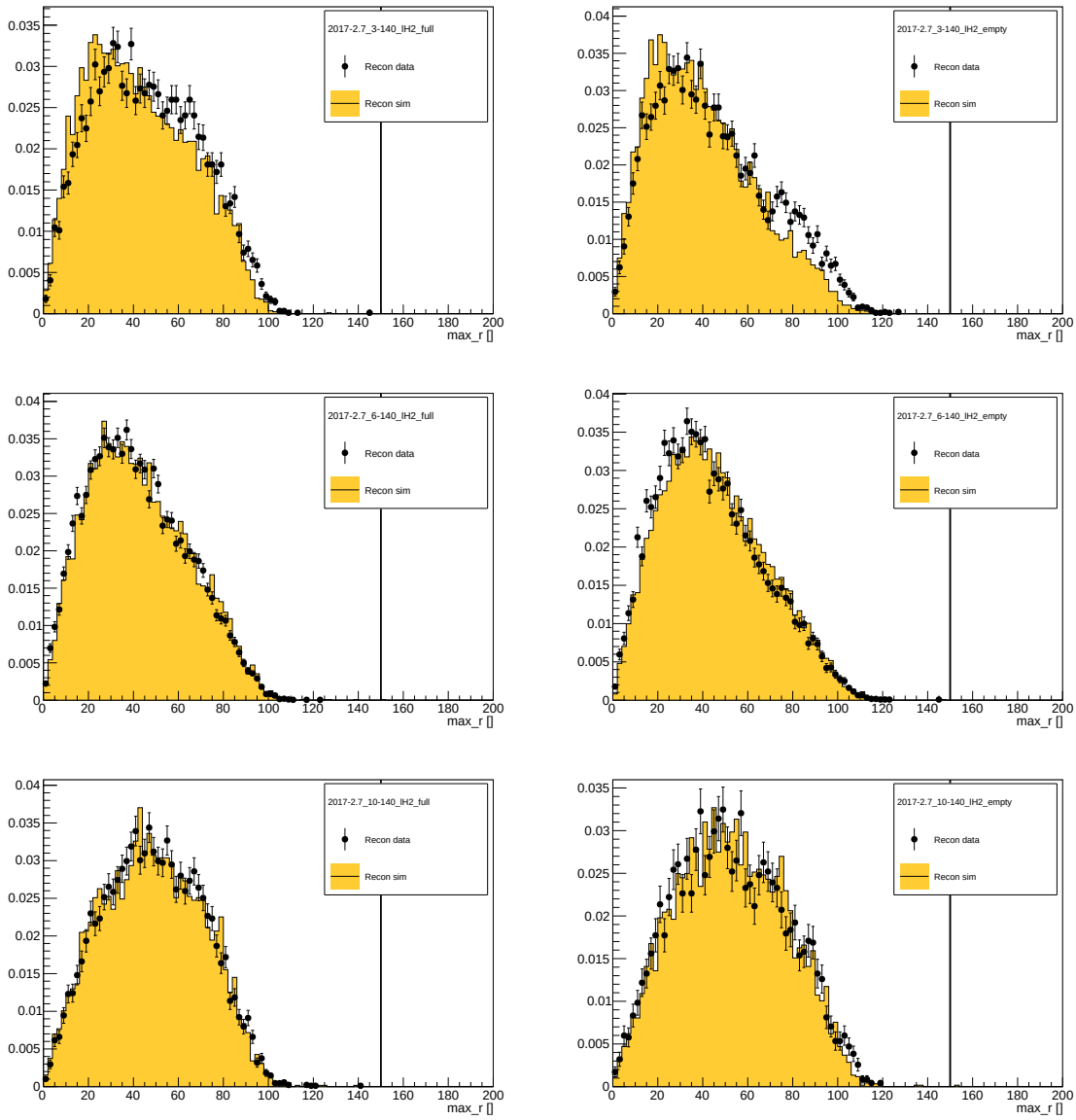

Figure 15: Max r.

9 Conclusions

Author: Rogers

blah blah.

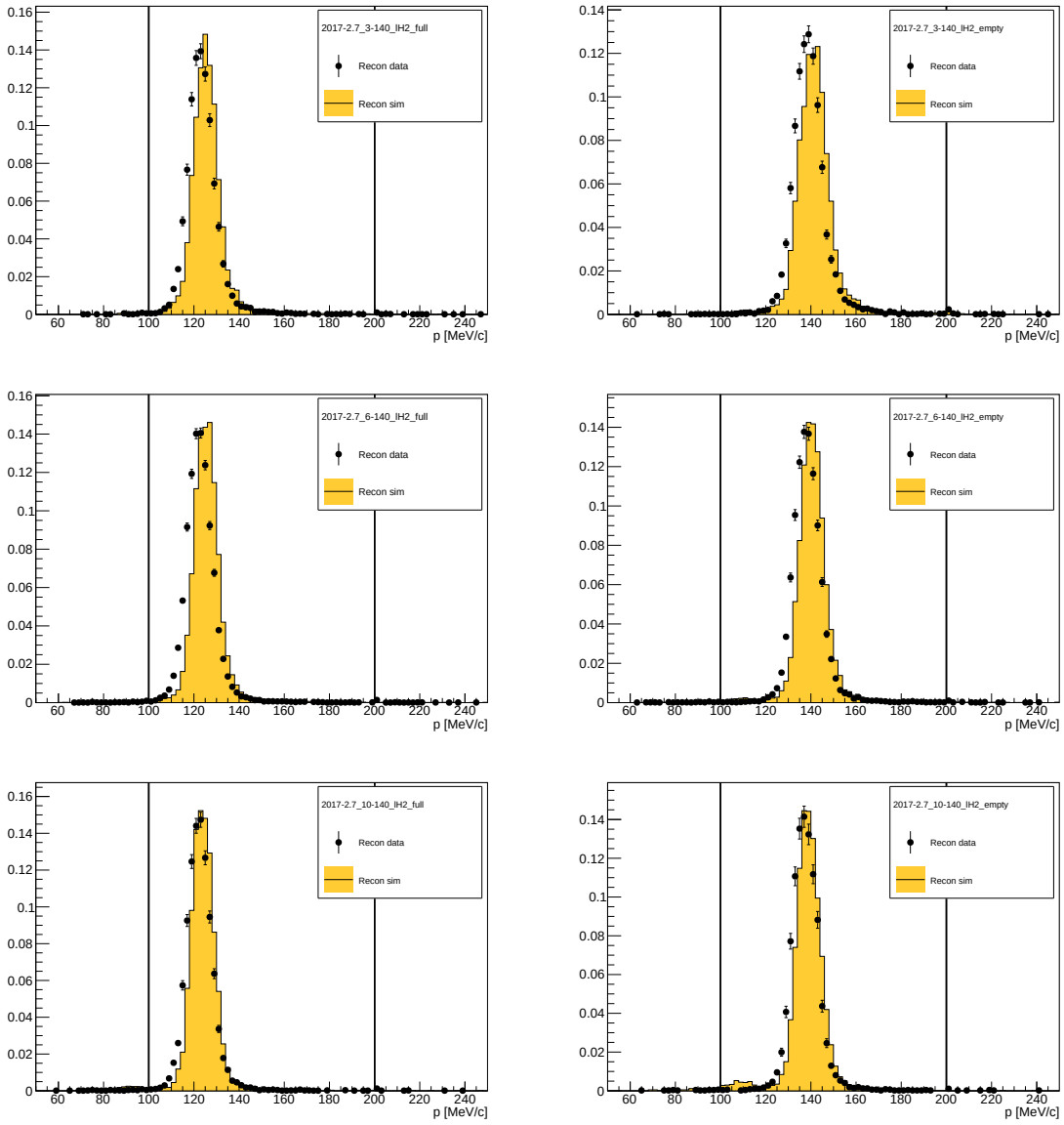

Figure 16: TKD momentum.

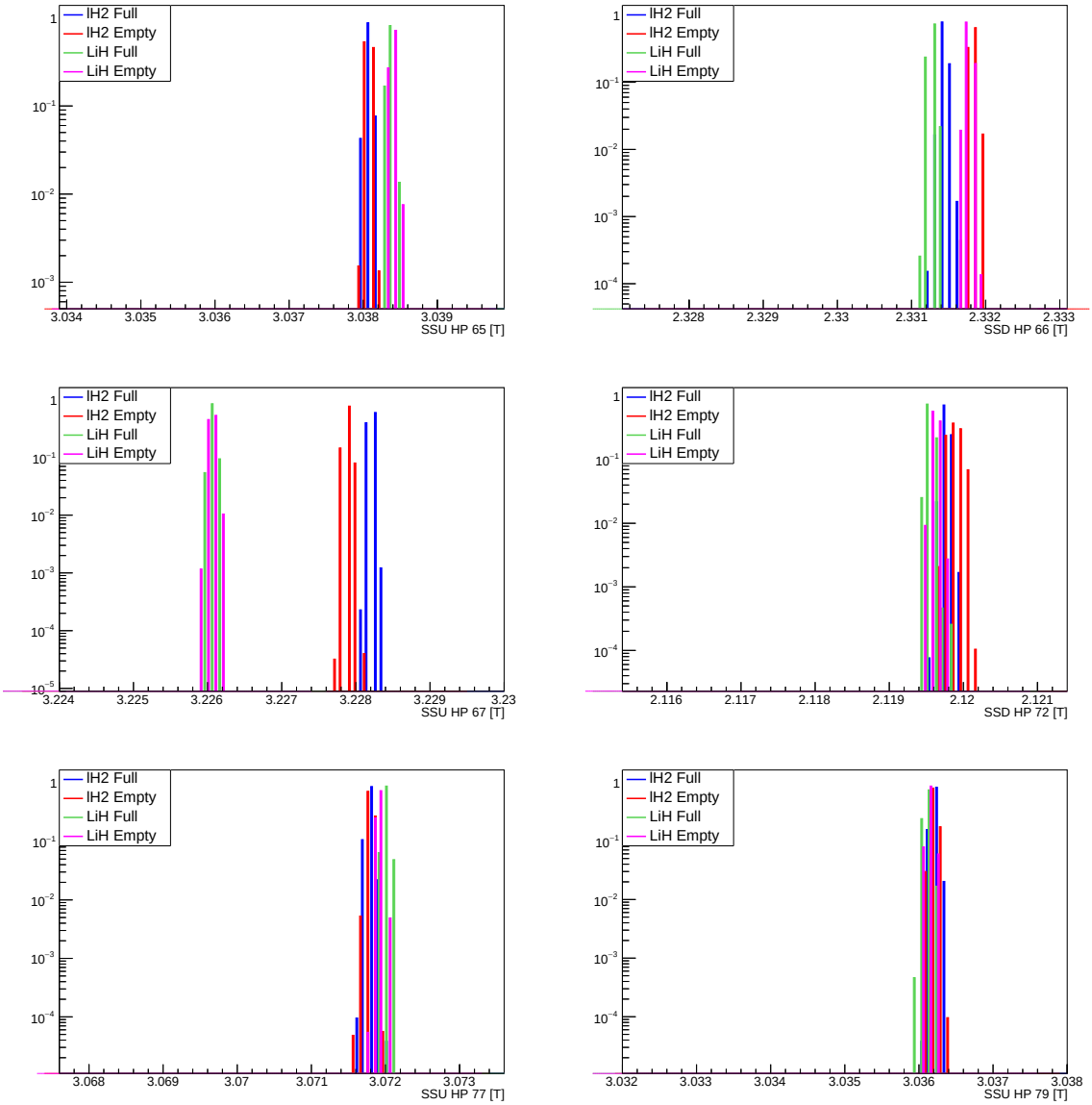

Figure 17: Hall probe readings for the two datasets across the entire period where data was taken.

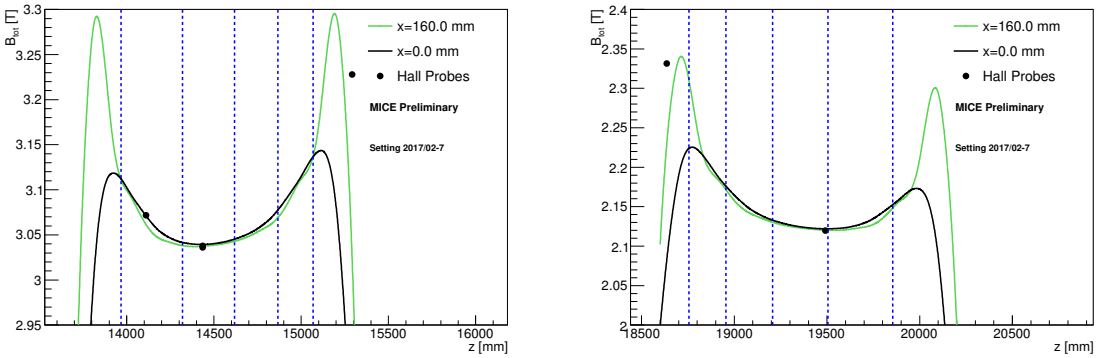

Figure 18: Hall probe readings compared to the field model used for reconstruction and track extrapolation. Blue dashed lines show the position of the tracker stations.

Figure 19: Estimated TOF resolution.

References

R. Roser, A. Name†
Fermilab, P.O. Box 500, Batavia, IL 60510-5011, USA
† *Also at another institute*

K. Long
Physics Department, Blackett Laboratory, Imperial College London, Exhibition Road, London, SW7 2AZ, UK